

# Monitoring *RXTE* Observations of Markarian 348: the origin of the column density variations

A. Akylas<sup>1,2</sup>, I. Georgantopoulos<sup>1</sup>, R. G. Griffiths<sup>3</sup>, I. E. Papadakis<sup>4</sup>, A. Mastichiadis<sup>2</sup>,  
R. S. Warwick<sup>3</sup>, K. Nandra<sup>5</sup>, D.A. Smith<sup>6</sup>

<sup>1</sup> *Institute of Astronomy & Astrophysics, National Observatory of Athens, I. Metaxa B. Pavlou, Penteli, 15236, Athens, Greece*

<sup>2</sup> *Physics Department University of Athens, Panepistimiopolis, Zografos, 15783, Athens, Greece*

<sup>3</sup> *Department of Physics and Astronomy, University of Leicester, Leicester LE1 7RH*

<sup>4</sup> *Physics Department University of Crete, 73010, Heraklion, Greece*

<sup>5</sup> *Laboratory for High Energy Astrophysics, Code 660, NASA/Goddard Space Flight Center, Greenbelt, MD20771, U.S.A.*

<sup>6</sup> *University of Maryland, College Park, MD 20742, U.S.A.*

28 October 2018

## ABSTRACT

We analyze 37 *RXTE* observations of the type 2 Seyfert galaxy Mrk348 obtained during a period of 14 months. We confirm the spectral variability previously reported by Smith et al., in the sense that the column density decreases by a factor of  $\sim 3$  as the count rate increases. Column density variations could possibly originate either due to the random drift of clouds within the absorption screen, or due to photoionization processes. Our modeling of the observed variations implies that the first scenario is more likely. These clouds should lie in a distance of  $>2$  light years from the source, having a diameter of a few light days and a density of  $> 10^7 \text{ cm}^{-3}$ , hence probably residing outside the Broad Line Region.

## Key words:

galaxies:active-quasars:general-X-rays:general

## 1 INTRODUCTION

Monitoring observations are a powerful tool in the study of the nuclear environment of type 2 Seyfert galaxies. Although the presence of X-ray flux variability in Seyfert-2 galaxies is well established (eg Georgantopoulos & Papadakis 2001 and references therein), our understanding of their spectral variations remains limited. Nevertheless, monitoring of the X-ray spectra of a few bright Seyfert-2 galaxies have revealed some intriguing results. For example, Warwick et al. (1988) first reported variations of the column density in ESO 103-G35. Using *EXOSAT* data, they found a decrease in the column density by a factor of  $\sim 1.7$  in a period of 90 days. Warwick et al. (1993) found column density variations in NGC 7582 by a factor of  $\sim 3$  over an interval of about 4 years, using *Ginga* data. They attributed these variations to motions of clouds near the central source. Investigation of the spectrum of NGC 7582 based on *ASCA* data by Xue et al. (1998) confirmed the existence of significant column density variations (by a factor of  $\sim 2$ ) over a timescale of 2 years. Variability analysis of column density variations in large samples of Seyfert-2 galaxies has been performed by Malizia et al. (1997) and Risaliti, Elvis & Nicastro (2002) using mainly literature data. They find variation of the col-

umn density in time scales of a few months up to several years.

Systematic monitoring observations only became feasible with the *RXTE* mission. In particular, Georgantopoulos et al. (1999), Georgantopoulos & Papadakis (2001), Smith, Georgantopoulos & Warwick (2001) present monitoring observations of several Seyfert-2 galaxies (Mrk3, ESO 103-G35, IC 5063, NGC 4507, NGC 7172 and Mrk 348) spanning time periods from about seven days to seven months. They found statistically significant spectral variations in all cases. In some objects the variations appear to be caused by intrinsic power-law slope changes whereas in others column density variations dominate.

In this paper we present an analysis of 37 *RXTE* observations of the Seyfert 2 galaxy Mrk348. Previously Smith et al. (2001) have reported the results from 12 *RXTE* observations covering a period of six months. Here we use an expanded sample of 37 *RXTE* monitoring observations of Mrk 348 (including the 12 reported by Smith et al. 2001), spanning a time interval of 14 months, to investigate further the nature of the X-ray spectral variability exhibited by this source. More specifically, we investigate whether photoionization of the absorbing screen or alternatively motion of

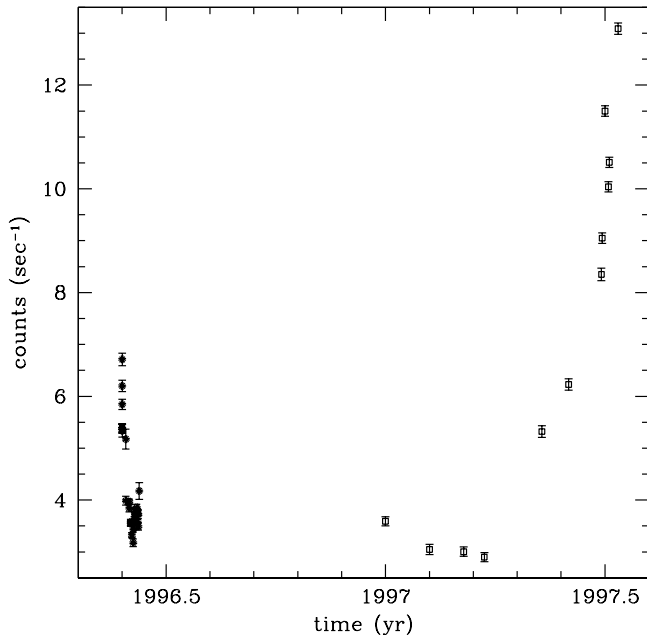


**Figure 1.** The background subtracted count rate versus time for the 37 observations of Mrk348. The open squares denote the observations of Smith et al. (2001)

clouds along the line of sight can reproduce the observed spectral variability.

## 2 THE DATA

We use 37 observations of Mrk348 obtained with the Rossi X-ray Timing Explorer (*RXTE*) mission. The data are spanning a period of  $\sim 14$  months from May 24, 1996 to July 12, 1997. Each observation lasts typically 2500-5000 sec. Here we present data from the Proportional Counter Array (PCA, Glasser, Odell & Seufert 1994) instrument only. We use PCA units 0 to 2. The data from the other two units were discarded as these were turned off on some occasions. We extract 3-20 keV spectra from only the top layer in order to maximize the signal to noise ratio. The data were selected using the standard screening criteria. The background subtraction was done using the PCABACKEST v2 routine of FTOOLS which takes into account both cosmic and internal background using the latest L7 model (see Smith et al. 2001 for a detailed description).

The background subtracted light curve is presented in Fig 1. In particular the count rate of the source increases by a factor of  $\sim 5$  in the last few months. In the 1996 data the variations present half the above amplitude in a period of  $\sim 15$  days.

## 3 SPECTRAL ANALYSIS

### 3.1 Neutral absorption models

We use the XSPEC v11.0 software package in our spectral fitting analysis. In order to improve the signal-to-noise ratio,

we combine individual spectra obtained within up to four days. In this way we obtain 13 spectral datasets (9 of which overlap with the data analysed by Smith et al. 2001). Errors quoted correspond to the 90 per cent confidence level for one interesting parameter. All the energies refer to the observer's rest frame.

We perform joint fits in the 13 combined observations in order to derive the best fit model. We fit the data using a simple absorbed power-law model plus a Gaussian line ( $\sigma = 0.1$  keV) to account for Fe K emission. Both the column density and the photon index were tied to a single value and only the normalization of the power-law was allowed to vary freely. This model provides an unacceptable fit to the data ( $\chi^2 = 2310/568$ ). Therefore we set the  $N_H$  parameter free for all the observations. We obtain a good fit with  $\chi^2 = 480/556$ . Furthermore we investigate possible variations of the photon index. We keep  $N_H$  tied to a single value and let the photon index parameter to vary free for all the observations. The value of  $\chi^2$  (538/556) implies that this is a good fit. We also allow both the column density and the photon index parameters to vary freely. This gives a statistically significant reduction in  $\chi^2$  (390/544). We conclude that both column density and photon index variations exist.

Apparent variations of the photon index could be due to the presence of a reflection component (see for example Georgantopoulos et al. 1999 in the case of Mrk3). To test this assumption we include in our model a reflection component (*PEXRAV* model in XSPEC,  $R=-1$ ,  $E_{\text{cut}}=150$  keV, solar abundances). We repeat the same analysis as above. First we let only the column density and the power-law normalization to vary freely. The power-law and the reflection component photon index were tied to a single value for all the observations. The normalization of the reflection component was tied to a single value. We obtain a good fit with  $\chi^2 = 365/555$ . The best fit photon index value was  $1.85^{+0.02}_{-0.02}$ . Therefore, in the subsequent analysis, we fix the reflection photon index to 1.85. In addition to  $N_H$  we also let the power-law photon index to vary freely. We find  $\chi^2 = 350/543$ . The reduction in  $\chi^2$  was less than 15 for 12 additional parameters compared to the previous model ( $\Gamma$  fixed to a common value and  $N_H$  free) which is not statistically significant. We also let the normalization of either the Fe line or the reflection component to vary freely between the observations. The fit is not improved at a statistically significant level:  $\Delta\chi^2 \approx 6$  and 10 respectively for 12 additional parameters. Therefore we conclude that the only varying parameters between the observations were the power-law normalization and the column density.

Hereafter, we call the variable column density absorbed power-law plus a Gaussian line and a constant reflection component as the "standard" model. In Fig. 2 we plot the column density variations as a function of the observation time. The best fitting model parameters are listed in Table 1. They are in good agreement with the results of Smith et al. (2001). The ratio of the reflected to the total flux (3 to 20 keV) varies between 0.09 and 0.3. The best fitting line energy is  $E=6.1^{+0.1}_{-0.1}$  keV ( $\sigma=0.1$  keV). This energy is below that expected for cold iron. As noted by Smith et al. (2001) the discrepancy could be caused by uncertainties in the instrument response around the XeL edge. The EW of the Fe line varies between 70 and 340 eV, being anti-correlated with the power-law flux variations.

Recently, evidence for a double absorbing screen which partially or fully covers the nucleus in several type 2 Seyfert galaxies has emerged (eg Turner et al. 2000). Smith et al. (2001) found that a double screen model consisting of a variable column density and a fixed partial coverer provides a good description to the data of Mrk348. Here, we use a slightly different screen absorption model consisting of a neutral variable covering fraction and a constant column density (models *ZPCFA* and *WA* in XSPEC). In this model, the first variable screen could account for clouds orbiting close to the nucleus while the outer constant screen may be associated with the molecular torus. The best fitting results for this model are listed in Table 1. The  $\chi^2$  value (322/552 d.o.f) implies that this model provides the best description to our data so far. The constant column density is  $N_H = 12^{+1}_{-1} \times 10^{22} \text{ cm}^{-2}$  while the variable screen has  $N_H = 28^{+1}_{-1} \times 10^{22} \text{ cm}^{-2}$  and a covering fraction between 0.05 and 1.

### 3.2 Photoionization models

Fig. 3 shows the best fitting column density values for the standard model as a function of the source unobscured luminosity (crosses). There appears to be an anti-correlation in the sense that the column density decreases with increasing flux. This anti-correlation is introduced mainly by the last three points and is found to be significant at the 90 percent confidence level using the Kendall's test (Press et al. 1986). Such a behaviour suggests that the column density variations may be caused by photoionization processes. In order to check this possibility we use the ionized absorber model *ABSORI* (Magdziarz & Zdziarski 1985) in XSPEC instead of the neutral partial covering fraction absorption model *ZPCFA*.

We use again a double absorption screen model. Both absorbers are assumed to fully cover the source. One absorber is neutral (with column density  $N_H^1$ ) while the other ( $N_H^2$ ) is partially ionized and variable as  $\xi = L/nR^2$ . Hence the *effective* column density ( $N_H^2$ ) varies with luminosity. We also assume  $\Gamma = 1.85$ , a Gaussian line ( $E=6.1 \text{ keV}$  and  $\sigma = 0.1 \text{ keV}$ ) and an edge at  $5.38 \text{ keV}$ .

The best fitting results are listed in Table 1. The neutral and ionized column densities are  $N_H^1 \sim 8 \times 10^{22} \text{ cm}^{-2}$  and  $N_H^2 \sim 25 \times 10^{22} \text{ cm}^{-2}$  respectively. The ionization parameter varies roughly between 0 and 450 while the best fitting temperature is  $\sim 5 \times 10^5 \text{ K}$ . Although this model provides an acceptable fit to the data ( $\chi^2=450$  for 553 d.o.f), it yields an increase in  $\chi^2$  by  $\sim 130$  compared to the double neutral absorption model discussed earlier.

We have cross-checked the above results using the photoionization code XSTAR (Kallman & Krolik 2000) instead of the *ABSORI* model. The XSTAR calculates the physical conditions, emission and absorption spectra of photoionized gases. We created absorption table models representing the fraction of incident continuum emerging from a photoionized screen with a range of photoionization parameters, ( $\log \xi = -3$  - 3) and column densities ( $N_H = 6 \times 10^{22} - 4 \times 10^{23} \text{ cm}^{-2}$ ). A constant density of  $n=10^9$  hydrogen atoms/ions  $\text{cm}^{-3}$  was used and the gas temperature was fixed at  $10^6 \text{ K}$ . We fit the data using the same model as above, substituting the *ABSORI* component with the absorption table model produced by XSTAR. The best fitting values are

listed in Table 1. The value of the neutral column density is  $N_H^1 \sim 8 \times 10^{22} \text{ cm}^{-2}$  and the value of the total column density subject to photoionization is  $N_H^2 \sim 27 \times 10^{22} \text{ cm}^{-2}$ . The ionization parameter varies roughly between 0.001 and 350. These values are in agreement with the *ABSORI* model results.

Both *ABSORI* and XSTAR results suggest that in the photoionization scenario the medium subject to the intense photoionizing flux has a column density of  $\sim 27 \times 10^{22} \text{ cm}^{-2}$ . In Fig. 3 the solid line represents the column density of a neutral gas giving the equivalent absorption (within the limitations of both the *RXTE* spatial resolution and the crude modelling) as the photoionized medium. In order to convert the ionization parameters ( $\xi = L/nR^2$ ) derived from XSTAR to luminosities, we have assumed  $nR^2 \approx 10^{42} \text{ cm}^{-1}$ . Different values of  $nR^2$  will move the theoretical curve in Fig. 3 along the x-axis.

Although the relatively poor  $\chi^2$  values we obtain rather argue against photoionization models, the key test is the presence of absorption edges due to ionized Fe. In these models, the observations with low effective  $N_H$  should correspond to a highly ionized state. Therefore ionized edges should be present in their spectra. We fit (using the "standard" model) all the observations separately in order to investigate the existence of an ionized edge. The energy of the edge was allowed to vary between 7.1 and 8 keV. Even in the case where the column density was at the lowest state we find no evidence for such a component ( $\Delta\chi^2 < 1$ ,  $E_{\text{edge}} = 7.26 \text{ keV}$  and  $0 < \tau < 0.1$ ). However, this could be due to the relatively low resolution of the PCA which makes difficult to test the presence of such features. Therefore we checked for an Fe edge in the *ASCA* observation of Mrk348, obtained in August 4, 1995. We fit simultaneously both SIS and GIS spectral files (exposure time  $\sim 50 \text{ ks}$ ) obtained from the Tartarus AGN database (Turner et al. 1998). The best fit model ( $\chi^2 = 220/180 \text{ d.o.f}$ ) consists of a power-law with  $\Gamma = 0.5^{+0.2}_{-0.2}$  absorbed by a column density of  $N_H \sim 7 \times 10^{22} \text{ cm}^{-2}$ , plus a Gaussian line at  $6.4 \text{ keV}$  ( $\sigma = 0.01 \text{ keV}$ ). There is no statistically significant evidence for the existence of an ionized edge. Indeed, we obtain  $\Delta\chi^2 < 3$  for two additional parameters when such a feature is included in the fit. The best fitting values are  $E = 7.2^{+1.0}_{-1.7} \text{ keV}$  and  $\tau = 0.20^{+0.15}_{-0.15}$ .

### 3.3 Cloud models

Assuming, based on the above results, that a photoionization scenario alone cannot properly describe the observed column density variations we further try to derive constraints on the size, the velocity and the density of the neutral clouds which could alternatively be responsible for the  $N_H$  variations. More specifically, we assume that the column density variations are caused by the motion of a *single* cloud through the line of sight. We further assume that this is a spherical, (with diameter  $D$ ) neutral or weakly ionized cloud, ( $\xi \sim 1$ ) moving in a keplerian circular orbit around the central mass. Then, the velocity and crossing time of the cloud are given by  $v = (GM/r)^{1/2}$  and  $t = D/2v$ . Combining the above two equations with the definition of the ionization parameter, the density and the radius of this cloud are given by  $n_{10} = 129 \Delta N_{22}^{4/5} L_{42}^{1/5} / (t^{4/5} M_8^{2/5} \xi^{1/5})$

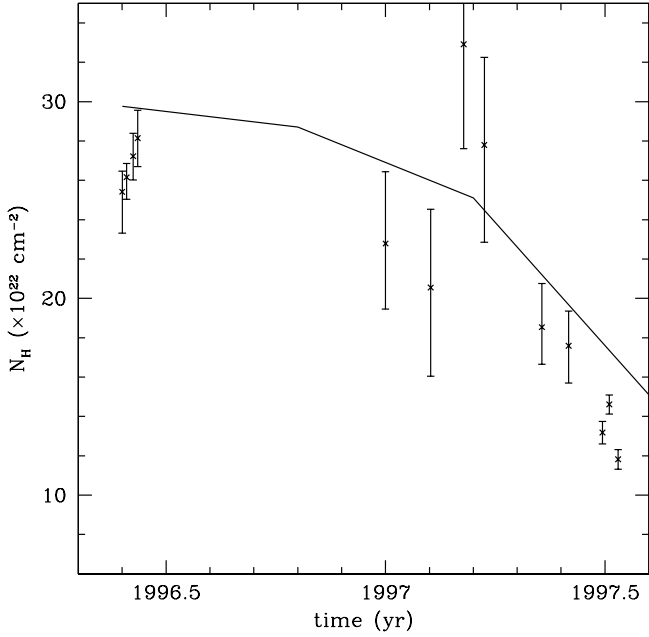


**Figure 2.** The  $N_H$  variations of the standard model (crosses) plotted as a function of the observation time. The solid line model describes the expected column density variations due to the circular motion of a spherical cloud around the source

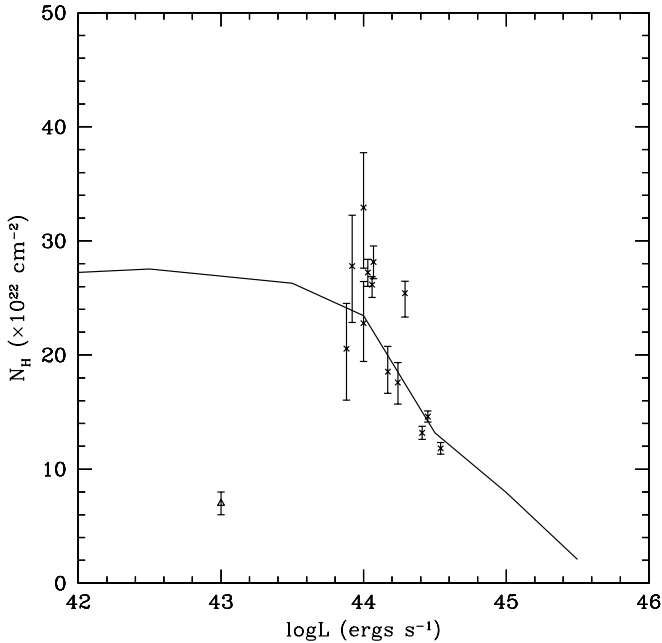


**Figure 3.** The observed column density variations, obtained from the standard model as a function of the unobscured luminosity in the 0.0136–13.6 keV band (crosses). The solid line denotes the XSTAR theoretical curve describing the changes in the column density due to ionization. The triangle shows the results from the 1995 *ASCA* observation using the standard model

and  $r_{16} = 0.09t^{2/5}M_8^{1/5}L_{42}^{2/5}/(\Delta N_{22}^{2/5}\xi^{2/5})$ , (Griffiths 1999, Risaliti et al. 2002) where  $n_{10}$  is the density of the cloud in units of  $10^{10} \text{ cm}^{-3}$ ,  $r$  is the radius of its orbit in units of  $10^{16} \text{ cm}$ ,  $\Delta N_{22}$  is the change in the column density in units of  $10^{22} \text{ cm}^{-2}$ ,  $t$  is the time scale of the  $N_H$  variations,  $L$  is the unobscured luminosity in units of  $10^{42} \text{ ergs s}^{-1}$  and  $M_8$  is the mass of the black hole in units of  $10^8 M_\odot$ . The mass of Mrk348 (Nishiura & Taniguchi 1998) is  $5 \times 10^8 M_\odot$ . For  $t=4 \times 10^7 \text{ sec}$ ,  $\Delta N_{22} = 14$  (based on Fig. 2) and  $L=50$ , we obtain  $n \sim 10^7 \text{ cm}^{-3}$  and  $r \sim 2.3 \text{ light years}$ . Then  $v \sim 1700 \text{ km s}^{-1}$  and  $D_{cloud} \sim 0.014 \text{ light years}$ . In Fig. 2 the solid line describes the expected column density variations due to the motion of a spherical cloud with the above properties in the line of sight. In this model a constant column density of  $\sim 10^{23} \text{ cm}^{-2}$ , (due to the constant absorption screen found in the best fit model) was also added. Note that the above calculations give only a rough estimate for the distance of the cloud. In reality, the value of the ionization parameter remains unknown and introduces some uncertainty in the estimate of the cloud distance. Using a lower limit value for  $\xi$  of  $10^{-3}$  we find upper limits of  $r \sim 37 \text{ light years}$  and  $n \sim 4 \times 10^7 \text{ cm}^{-3}$  for the distance and the density respectively. The Broad Line Region (BLR) in Active Galactic Nuclei lies approximately from several light months to several light years and its density is  $\sim 10^9 \text{ cm}^{-3}$ . The velocities in the BLR vary between  $1000\text{--}10000 \text{ km s}^{-1}$ . The Narrow Line Region lies in much larger distances (up to 1 kpc) and its density is  $\sim 10^3 \text{ cm}^{-3}$ . Characteristic velocities of this region are  $\sim 500 \text{ km s}^{-1}$  (Peterson 1993). Therefore in the case of Mrk348 the clouds responsible for the column density variations should lie outside the BLR. Note that such clouds are quite different from the molecular clouds observed in our Galaxy which have a much larger diameter (several light years) and a much smaller density (typically  $10^2 \text{ cm}^{-3}$ ).

One possible problem with the cloud scenario is the observed anti-correlation between the column density and the unobscured luminosity (Fig.3). Indeed, in the simple cloud model there should be no such anti-correlation as the *unobscured* luminosity is only driven by changes in the accretion rate and is hence unrelated to the cloud motion and properties. In our case, the increase of the luminosity while  $N_H$  drops could be purely coincidental (eg the luminosity of the source increased while the cloud was moving progressively out of the line of sight). Indeed the *ASCA* point (triangle in Fig 3) suggests that the column density has drifted (due to motion of clouds) at least between the *ASCA* and *RXTE* epochs and therefore this correlation should be coincidental.

## 4 CONCLUSIONS

We model the X-ray spectral variability of Mrk348 by analyzing 37 *RXTE* observations over a period of 14 months. The present work extends our previous study (Smith et al. 2001) where 12 observations spanning a period of 6 months were used. We find that the column density decreases by a factor of 3 with increasing flux, confirming our previous results. These column density variations could arise either due to the random drift of clouds within the absorption screen or due to photoionisation processes.

Our modelling shows that photoionization alone cannot

easily reproduce the observed column density variations. In particular, both the *ABSORI* and the *XSTAR* models yield a worse fit to the data compared to the double neutral absorber model. This is further supported by the *ASCA* observation which does not show any significant evidence for an ionized edge.

Alternatively a model which assumes that a neutral or a weakly ionized cloud is moving in front of the source can reproduce successfully the column density variations. If we assume that the observed  $N_H$  variations are caused by a single spherical cloud which moves in a circular orbit, then, this cloud should lie in a distance of  $>2$  light years from the source having a density of  $> 1 \times 10^7 \text{ cm}^{-3}$ . These values are probably characteristic of a region outside the BLR.

Future observations with the XMM mission, which combines large effective area and excellent spectral resolution will shed more light on the origin of the obscuring screen in Seyfert 2 galaxies.

## 5 ACKNOWLEDGMENTS

We would like to thank the referee G. Risaliti for many useful comments. This research has made use of data obtained from the High Energy Astrophysics Science Archive Research Center (HEASARC), provided by NASA's Goddard Space Flight Center.

## REFERENCES

- Georgantopoulos, I., Papadakis, I., 2001, MNRAS, 322, 218  
 Georgantopoulos, I., Papadakis, I., Warwick, R. S., Smith, D. A., Stewart, G. C., & Griffiths, R. G., 1999, MNRAS, 307, 815  
 Glasser, C. A., Odell, C. E., & Seufert S. E., 1994, IEEE Trans. Nucl. Sci., 41, 1343  
 Griffiths, R. G., 1999, PhD thesis, Univ. of Leicester  
 Kallman, T. R., Krolik, J. H., 2000, XSTAR: A spectral analysis tool, Version 2.0 of the User's Guide  
 Magdziarz, P., Zdziarski, A., 1995, MNRAS, 273, 837  
 Malizia, A., Bassani, J., Malaguti G., Palumbo G. G. C., 1997, ApJS, 113, 311  
 Peterson, B. M., 1993, PASP, 105, 247  
 Press, W. H., Flannery, B. P., Teukolsky, S. A., Vetterling W. T., 1986, Numerical Recipes, The art of Scientific Computing, Cambridge Univ. Press, Cambridge  
 Risaliti, G., Elvis, M., Nicastro, F., 2002, astro-ph/0107510  
 Nishiura, S., Taniguchi, Y., 1998, ApJ, 499, 134  
 Smith, D. A., Georgantopoulos, I., Warwick, R. S., 2001, ApJ, 550, 635  
 Turner, T. J., Nandra, K., Turcan, D., George, I. M., 1998, in Paul, J., Montmerle, T., Aubourg E., eds, 19th Texas Symposium on Relativistic Astrophysics and Cosmology, CEA Saclay, p. 441  
 Turner, T. J., Perola, G. C., Fiore, F., Matt, G., George, I. M., Piro, L., Bassani, L., 2000, ApJ, 531, 245  
 Warwick, R. S., Pounds, K. A., Turner, T. J., 1988, MNRAS, 232, 551  
 Warwick, R. S., Sembay, S., Yaqoob, T., Makishima, K., Ohashi, T., Tashiro, M., Kohmura, Y., 1993, MNRAS, 265, 412  
 Xue, S. J., Otani, C., Mihara, T., Cappi, M., Matsuoka, M., 1998, PASJ, 50, 519

**Table 1.** Best fit parameters

Model	$N_{\mathrm{H}}^1(\mathrm{cm}^{-2})$	$N_{\mathrm{H}}^2(\mathrm{cm}^{-2})$	covering fraction	$\Gamma$	$\xi$	EW(eV)	$\chi^2/\mathrm{dof}$
“standard”	$12_{-1}^{+1} - 32_{-4}^{+5}$	-	-	1.85	-	70-340	351/553
Double absorber (neutral)	$12_{-1}^{+1}$	$28_{-1}^{+1}$	0.05-1	1.85	-	70-300	322/551
Double absorber ( <i>slABSORI</i> )	$8_{-1}^{+1}$	$25_{-1}^{+1}$	-	1.85	0 – 450	80-410	450/551
Double Absorber (XSTAR)	$7_{-1}^{+1}$	$27_{-1}^{+1}$	-	1.85	0.01 – 350	75-400	460/551

<sup>1</sup> Neutral column density  $\times 10^{22}$ <sup>2</sup> Ionized or partial covering column density